Drug Design, Development and Therapy

Dovepress
open access to scientific and medical research

Open Access Full Text Article

ORIGINAL RESEARCH

Enhanced immunosuppressive effects of 3,5-bis[4 (diethoxymethyl)benzylidene]-1-methyl-piperidin-4-one, an α, β-unsaturated carbonyl-based compound as PLGA-*b*-PEG nanoparticles

This article was published in the following Dove Press journal:
Drug Design, Development and Therapy

Laiba Arshad[1]
Ibrahim Jantan[2]
Syed Nasir Abbas Bukhari[3]

[1]Department of Pharmacy, Forman Christian College (A Chartered University), Lahore, Pakistan; [2]School of Pharmacy, Faculty of Health and Medical Sciences, Taylor's University, Subang Jaya, Selangor, Malaysia; [3]Department of Pharmaceutical Chemistry, College of Pharmacy, Al Jouf University, Aljouf, Sakaka, Saudi Arabia

Background: 3,5-Bis[4-(diethoxymethyl)benzylidene]-1-methyl-piperidin-4-one (BBP), a novel synthetic curcumin analogue has been revealed to possess strong *in vitro* and *in vivo* immunosuppressive effects.

Purpose: The aim of present study was to prepare and characterize BBP-encapsulated polylactic-co-glycolic acid-block-polyethylene glycol (PLGA-*b*-PEG) nanoparticles and to evaluate its *in vivo* efficacy against innate and adaptive immune responses.

Methods: Male BALB/c mice were orally administered with BBP alone and BBP- encapsulated nanoparticles equivalent to 5, 10 and 20 mg/kg of BBP in distilled water for a period of 14 days. The immunomodulatory potential was appraised by determining its effects on non-specific and specific immune parameters.

Results: The results showed that BBP was successfully encapsulated in PLGA-b-PEG polymer with 154.3 nm size and high encapsulation efficiency (79%) while providing a sustained release for 48 hours. BBP nanoparticles showed significant enhanced dose-dependent reduction on the migration of neutrophils, Mac-1 expression, phagocytic activity, reactive oxygen species (ROS) production, serum levels of ceruloplasmin and lysozyme, immunoglobulins and myloperoxidase (MPO) plasma levels when compared to unencapsulated BBP. Enhanced dose-dependent inhibition was also observed on lymphocyte proliferation along with the downregulation of effector cells expression and release of cytokines, and reduction in rat paw oedema in BBP nanoparticles treated mice. At higher doses the suppressive effects of the BBP nanoparticles on various cellular and humoral parameters of immune responses were comparable to that of cyclosporine-A at 20 mg/kg.

Conclusion: These findings suggest that the immunosuppressive effects of BBP were enhanced as PLGA-*b*-PEG nanoparticles.

Keywords: αβ-unsaturated carbonyl-based compound, curcumin analogue, PLGA-*b*-PEG nanoparticles, immunosuppression, innate immune response, humoral immune response

Introduction

Curcumin is a polyphenolic, low molecular weight compound isolated from the rhizomes of turmeric (*Curcuma longa*).[1] This natural versatile compound has gained widespread popularity because of its remarkable applicability in prophylaxis as well as treatment of a variety of inflammatory conditions.[2,3] For the past three decades, studies have delineated that owing to curcumin's physiochemical limitations ie, poor water solubility, low bioavailability, chemical instability and rapid

Correspondence: Ibrahim Jantan
School of Pharmacy, Faculty of Health and Medical Sciences, Taylor's University, Lakeside Campus, 47500 Subang Jaya, Selangor, Malaysia
Tel +6 016 288 6445
Fax +6 035 629 5001
Email profibj@gmail.com

http://doi.org/10.2147/DDDT.S185191

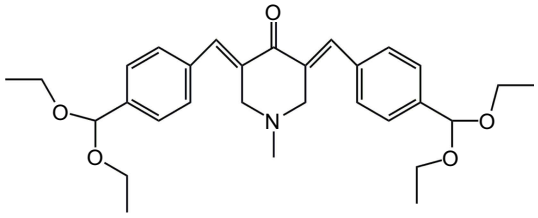

Figure 1 Chemical structure of 3,5-bis[4(diethoxymethyl)benzylidene]-1-methyl-piperidin-4-one.

metabolism, the in vivo application of curcumin is hindered, resulting in low potency and poor absorption characteristics.[4–6] Efforts to combat curcumin's in vivo limitations have generated the study of curcumin analogues and derivatives (natural, semisynthetic and synthetic) and novel delivery systems (nanoparticles) to increase its aqueous solubility, stability and bioavailability.[7] In this regard, different studies have reported the use of nanocarrier systems to deliver curcumin as well as its analogues and derivatives.[8–10]

Presently, a polymeric nanoparticle-based drug delivery system is being increasingly investigated.[11] Nanomaterial-based medicines offer a great potential in delivering drugs to the target sites and this delivery route is known to overcome many obstacles associated with delivery of free drugs and increase their pharmacological effects.[12,13] Polylactic-co-glycolic acid-block-polyethylene glycol (PLGA-*b*-PEG) polymeric nanoparticles employing PLGA-PEG block copolymer, is a delivery system with two model polymers, PLGA and PEG, in which PEG overcomes the demerits, associated with PLGA nanoparticles when used alone. Also PLGA-PEG nanoparticles have the potential advantage of hydrophilic character as well as reducing the opsonization and increasing the plasma circulation time of nanoparticles during in vivo application.[14,15]

Recently, we have reported a synthetic analogue of curcumin possessing an α, β-unsaturated carbonyl moiety, 3,5-bis[4-(diethoxymethyl)benzylidene]-1-methyl-piperidin-4-one (BBP) as a potent immunosuppressive agent (Figure 1). It has remarkably inhibited the in vitro phagocytosis process by granulocytes.[16] The immunosuppressive potential of this potent structurally modified compound has also been investigated on the eclectic parameters of nonspecific and specific cellular and humoral immunity in an animal experimental model.[17] Our previous findings encouraged us to prepare and characterize oral polymeric PLGA-PEG nanoparticles of synthetic curcumin analogue (BBP) and to compare its immunosuppressive effects with unencapsulated BBP on selected parameters of specific and nonspecific immune responses in BALB/c mice.

Materials and methods

Chemicals and reagents

PLGA-*b*-PEG (polylactic co-glycolic acid- polyethylene glycol) and pluronic F-68 were purchased from Sigma-Aldrich Chemicals Co. Ltd. (St Louis Missouri, USA). Acetonitrile was purchased from J.T. Baker Avantor Performance Materials, Inc. (Phillipsburg, NJ, USA) Lipopolysaccharide (LPS), concanavalin A (Con-A), Roswell Park Memorial Institute medium (RPMI)-1640 and sheep red blood cells (sRBCs) were obtained from Innovative Research, Inc. (Sarasota, FL, USA). FBS was obtained from PAA Laboratories (GE Healthcare UK Ltd, Little Chalfont, UK). Pharm Lyse™ lysing solution, allophycocyanin (APC)-conjugated anti-mouse CD8, APC-H7-conjugated CD4, FITC-A conjugated CD11b, PE-A conjugated CD18 and IgG-FITC were obtained from BD Biosciences (Franklin Lakes, NJ, USA). Cytoselect 24-well cell migration assay kits were obtained from Cell Biolabs, Inc. (San Diego, CA, USA). Ceruloplasmin and lysozyme kit was supplied by Wuhan Biotech Co., Ltd (Wuhan, China). Abcam Biotechnology Company (Cambridge, UK) supplied myeloperoxidase (MPO) ELISA kit. IgG and IgM ELISA kits were obtained from Life Diagnostics, Inc., (West Chester, PA, USA). Cyclosporine, ^{3}H-thymidine (0.5 μCi/well), and scintillation cocktail (Ultima Gold MV) were purchased from Perkin Elmer, Inc. (Waltham, MA, USA). IL-2, IL-4 and IFN-γ ELISA kits were purchased from R&D Systems Inc., (Minneapolis, MN, USA). A phagotest kit and a phagoburst kit was obtained from Glycotope Technology (Berlin, Germany).

Preparation of BBP-encapsulated PLGA-*b*-PEG nanoparticles

Polymeric PLGA-*b*-PEG nanoparticles were prepared by following the method of Fessi et al with slight modification through the nanoprecipitation technique.[18] Briefly, two phases were prepared separately ie organic phase and aqueous phase. The organic phase comprised of the synthetic analog, BBP (0.05%) and PLGA-*b*-PEG polymer (1%) which was dissolved in organic solvent, acetonitrile (30%). Then, 0.1% pluronic F-68 was added in distilled water to form the aqueous phase. The organic phase was added dropwise to the aqueous

phase and mixed under sonication for 30 minutes. Finally, the solution was evaporated by allowing it to stir uncovered for 2–3 hour at room temperature and centrifuged at 15,000 rpm for 15 minutes. The resulting nanoparticles were freeze-dried (Scanvac cool safe 110–4 system H031857, Vassingerad, Lynge, Denmark).

Characterization of nanoparticles

The nanoparticles were characterized in terms of particle size, zeta potential and polydispersity index (PDI) by using Zetasizer ZS-90 (Malvern, UK). Freeze-dried nanoparticles were reconstituted with distilled water, poured into quartz cuvettes and placed inside the sample chamber of nanosizer while the capillary cell was employed for measuring zeta potential. The measurements were performed in triplicate and the results are shown as mean ±SD In addition, the morphological characteristics of the prepared nanoparticles were investigated by using a transmission electron microscopic (TEM) analysis (FEI TECNAI G2 SPIRIT BIOTWIN, Hillsboro, OR, USA) at 120 kV. A drop of reconstituted nanoparticles was placed on a glow discharged 400-mesh carbon coated microscopic grid and stained using 0.1% phosphotungstic acid. The grid was viewed under different resolutions of TEM and the results were reported as micrographic images at 500 nm.

Encapsulation efficiency (% EE) and loading capacity (% LC)

The percentage of synthetic analogue (BBP) incorporated during nanoparticle preparation was determined using a UV-Vis spectrophotometer (UV 1800, Kyoto, Japan). The standard calibration curve was prepared by using different dilutions of BBP (100–700 µg/mL) in 25:75 ratio of acetonitrile and distilled water while the absorbance was measured at a wavelength of 370 nm. Finally, regression line of calibration as well as r^2 value were determined. Freeze-dried nanoparticles were reconstituted in distilled water and subjected to centrifugation at 15,000 rpm for 15 minutes at 4°C. The supernatant containing the unencapsulated drug was separated to determine the percent entrapment efficiency (% EE) and percent loading capacity (% LC).

In vitro release profile

The dialysis tube method was used to determine the release of synthetic compound from nanoparticles.[19] Two milliliters of nanoparticle solution equivalent to 2 mg of synthetic compound, BBP was put into a dialysis tubing cellulose acetate membrane (Sigma Aldrich Co.). The dialysis membrane was dialyzed against 30 mL of PBS, pH 7.4 and 2.1 to mimic human gastric and intestinal environment. The experiment was performed in a shaking water bath (37°C). At predetermined time points, 1.5 mL aliquots were taken and replaced by an equal volume of the dialysate to maintain the sink conditions. The concentration of synthetic compound was assessed by measuring the absorbance at 370 nm using a UV–visible spectrophotometer.

Fourier transform infrared spectroscopy (FTIR) study

The FTIR spectra of the drug (BBP), polymer (PLGA-*b*-PEG) and BBP-encapsulated nanoparticles were taken with a Perkin Elmer Spectrum 100 FTIR spectrophotometer. Small amounts of drug, polymer and freezedried nanoparticles were placed on an ATR crystal and the maximum force was applied by using an ATR pressure clamp to allow for optimum contact with the samples. Finally, each sample was scanned in a spectral region of 650–4000 cm^{-1} using a resolution of 4 cm^{-1} and 32 co-added scans were recorded.

Experimental animals

Male BALB/c mice (22–28 g) were obtained from the Laboratory Animal Resource Unit, Faculty of Medicine, Universiti Kebangsaan Malaysia (UKM, Cheras, Selangor, Malaysia). All procedures in animal studies were directed following a protocol approved by the UKM Animal Ethics Committee (No. FF/2016/IBRAHIM/28-SEPT./780-SEPT. -2016-MAC.-2018). During the experiment, animals were kept in a well-ventilated controlled room on a 12-hour light/12-hour dark schedule. The commercially available laboratory rodent diet along with water ad libitum was supplied to the animals. Animals were acclimatized for at least 1 week prior to being placed on study.

Study protocol

The study was conducted in three different experimental designs to determine selected parameters of specific and nonspecific immune responses in BALB/c mice. After being adapted to the environment for 1 week, the mice were randomly divided into 10 groups and each experimental group consisted of 6 animals. The first group of animals received a regular diet (normal control group).

The second group of animals received 1% sodium carboxymethyl cellulose (NaCMC) in distilled water (vehicle control group) whereas the third group received a known immunosuppressant, cyclosporine-A which was administered orally at a dose of 20 mg/kg BW (positive control group). The fourth group of animals was orally administered with blank nanoparticles (polymer only). The animals in the experimental groups (5–7) received curcumin analog, BBP alone after every 24 hours while the animals in the experimental groups (8–10) received BBP-encapsulated PLGA-*b*-PEG nanoparticles equivalent to 5, 10 and 20 mg/kg BW of BBP, after every 48 hours for 14 days. On day 15, the animals were humanely sacrificed and blood samples were collected to evaluate the effects of BBP nanoparticles on the phagocytic activity of neutrophils and to determine serum levels of lysozyme, ceruloplasmin and plasma (MPO levels. In the second experimental design, on day 0 of treatment, the mice were immunized intraperitoneally with 5.0×10^9 sRBCs/mL (a T cell-dependent antigen) as an antigenic stimulus. Prior to immunization, the sRBCs were washed three times with cold PBS and finally resuspended in PBS. At the end of the study, the mice were humanely killed and the spleen was collected for the analysis of T and B-cell proliferation and $CD4^+$ and $CD8^+$ expression in T cell subsets in splenocytes. The blood samples were also collected for the estimation of serum levels of cytokine production by activated T cells. In the third experimental study, the animals were also immunized with sRBCs on day 0 and the treated (with BBP alone and BBP nanoparticles)/untreated mice were investigated for delayed type hypersensitivity (DTH) and samples were collected for measuring serum immunoglobulins (IgG and IgM). Cyclosporine, a well-known immunosuppressant was used as a positive control in this study and the dose was decided based on previous studies,[20,21] while the safe doses for novel synthetic analog were selected based on toxicity study assessment from our previous study.[16]

Isolation of neutrophils from whole rat blood

The neutrophils were isolated from the whole blood of treated mice using a modified Histopaque® gradient technique.[22] Briefly, 2 mL of lymphoprep gradient (1,077 mg/mL) was placed into a 10 mL falcon tube and an equal volume of whole mice blood was carefully layered on the gradient without any break to the gradient and centrifuged at 400×g for 45 minutes. The high density neutrophils and erythrocytes were sedimented through the lymphoprep layer. Finally, the erythrocytes were lysed using Pharm Lyse™ lysing solution and incubated for 10 minutes. At the end of incubation, the falcon tube was centrifuged at 200×g for 5 minutes. The supernatant was aspirated carefully without disturbing the pellet and resuspended in PBS. The viability of cells was checked with trypan blue exclusion method.

Cell migration assay

The inhibitory effect of BBP and BBP nanoparticles on neutrophils migration was quantitatively measured by using modified method.[23] The neutrophils isolated from the nonimmunized mice whole blood were adjusted to a final concentration of 1.5×10^6 cells. A CytoSelect (San Diego, CA, USA) 24-well cell migration assay kit was used to perform the experiment. Initially, a total of 500 µL RPMI media comprising of chemotactic stimulant, 10% FBS was added to the lower chambers, while the cell suspension with 1.5×10^6 cells (300 µL) was added to the upper chamber of a 24-well tissue culture plate and incubated for 2.5 hours at 37°C. After the specified time interval, the inserts were shifted to the new wells containing cell detachment solution and again incubated (30 minutes) to remove cells from the bottom of the inserts. Finally, the inserts were discarded and dislodged cells were stained by adding the lysis buffer/CyQuant® GR dye solution (Eugene, OR, USA). The number of cells migrating to lower chambers was determined by a fluorescence plate reader.

CD11b and CD18 integrin expression on leukocytes

The Mac-1 expression assay was carried out by following the method of Ahmad et al with slight modification.[24] LPS (3.5 µg/mL) was added to aliquots (100 µL) of isolated neutrophils from mice whole blood and incubated at 37°C for 30 minutes. Thereafter, the tubes were simultaneously placed on ice and 10 µL of CD11b-FITC-A, CD18-PE-A were added to the mixture. Meanwhile, IgG- FITC was added as isotype control and tubes were incubated on ice for 60 minutes. Subsequently, the tubes were centrifuged at a speed of 250×g for 10 minutes and the supernatant was discarded while retaining the pellet. Finally, the cells were resuspended in PBS and the inhibition of adhesion molecule expression was analyzed by flow cytometer.

Phagocytic assay

The phagocytic activity assay was determined by using the commercially available phagotest assay kit. The isolated neutrophils from the whole mice blood (100 µL) was incubated with 20 µL of FITC *Escherichia coli* in shaking water bath at 37°C for 10 minutes. Thereafter, the samples were immediately transferred on ice to stop the process of phagocytosis followed by the addition of quenching solution. The sample tubes were centrifuged at 250×g for 5 minutes (4°C) after adding 3 mL of washing solution. Finally, 200 µL of DNA staining solution was added to each tube and vortexed. The phagocytic activity was analyzed by flow cytometer and was determined as the percentage of phagocytizing neutrophils.

Phagoburst assay

The quantitative determination of oxidative burst of isolated neutrophils was carried out by using a commercially available kit and assay was carried out following manufacturer's protocol. Briefly, 100 µL of neutrophil cell suspension was incubated with 20 µL FITC-labeled *E. coli* at 37°C for 10 minutes in order to stimulate the cells. Afterwards, 20 µL of substrate solution (dihydrorhodamine, DHR 123) was added to determine the percentage of phagocytic cells producing reactive oxidants and again incubated for 10 minutes. Finally, 200 µL of DNA staining solution was added and cells were analyzed by flow cytometry.

Plasma level of MPO enzyme

MPO levels in the plasma were assessed by using a commercially available MPO ELISA kit and the experiment was carried out as per manufacturer's protocol. Plasma was separated by centrifuging the whole blood collected from euthanized mice at 2,000×g for 5 minutes at 4°C and was investigated for MPO levels by measuring absorbance on a microplate reader.

Analysis of serum levels of lysozyme and ceruloplasmin

The effect of BBP and BBP nanoparticles on serum levels of lysozyme and ceruloplasmin was determined by using a commercially available kit. The whole mice blood was centrifuged at 5,000 rpm for 20 minutes at 4°C to separate the serum. The collected serum was kept at 20°C until the experiment was done. The assay was performed using the manual provided by the manufacturer.

Spleen cell suspension preparation

From the animals immunized with 5.0×10^9 sRBCs/mL intraperitoneally, the spleen was removed aseptically and the splenocyte suspension was prepared using the method of Arshad et al.[16] The spleen was washed with cold PBS and placed onto a nylon cell strainer (70 µm) and cut into small pieces. By using the plunger at the end of a syringe, the small pieces of spleen were pushed through the strainer and the cells were then washed with excess PBS. The cell suspension was centrifuged at 300×g for 5 minutes and supernatant was aspirated. To lyse the RBCs, the pellet was resuspended in 2 mL pre-warmed (at 37°C) Pharm Lyse™ lysing solution and for 3 minutes at 37°C. Finally, the cells were washed, supernatant was discarded and the pellet was resuspended in 1 mL of complete medium. By using the trypan blue exclusion method, the viability of cells was assessed.

T and B lymphocyte proliferation assay

The method described by George et al was used to perform the lymphocyte proliferation assay.[25] LPS and Con-A at different concentrations (5 and 10 µg/mL, respectively) were used to stimulate the splenocytes. Concisely, 4×10^5 cells/mL of spleen cell suspension in RPMI complete medium was incubated with or without aforesaid mitogens in 96-well plates (200 µL/well) for 48 hours. Afterwards, ^{3}H-thymidine (0.5 µCi/well) was incorporated in all wells and incubated for 24 hours. Upon completion of incubation period, by using a Nunc cell harvester (Rochester, NY, USA), the cells were harvested and 5 mL of scintillation fluid was added to determine the thymidine incorporation by a liquid scintillation counter (counts per minute). The results were expressed as the stimulation index (SI).

T lymphocyte phenotyping by flow cytometric analysis

With slight modification, the method previously described by Gupta et al was used.[26] Briefly, 50 µL of splenocytes cell suspension (1×106 cells/mL) was incubated with 10 µL of APC-conjugated anti-mouse CD8 and APC-H7-conjugated anti-mouse $CD4^+$ antibodies on ice for 30 minutes. Thereafter, the cell suspension was washed with cold PBS (2 mL) and centrifuged at 250×g for 5 minutes. Lastly, the supernatant was removed and the pellet was resuspended in 300 µL of PBS. Acquisition and analysis were performed with multicolor flow cytometry using Cell Quest Pro Software (San Jose, CA, USA). The results

were expressed in percentage of $CD4^+$ and $CD8^+$ expressions.

Measurement of Th1/Th2 cytokines

The serum levels of IL-2, IL-4 and IFN-γ from the treated and untreated mice were quantitatively determined using the commercially available ELISA kits (R&D Systems). The serum was separated from whole blood (collected under sterile conditions from the experimental animals) by centrifuging it at 2,000×g and 4°C for 20 minutes. The assay was performed using the standard protocol provided by the manufacturer. The results were determined within 30 minutes using a plate reader set to 450 nm.

Delayed type hypersensitivity reaction (DTHR)

The DTHR or footpad reaction was performed using a method described by Koffuor et al with minor modification.[27] Male BALB/c mice were divided into six groups with 6 animals in each group. On day 0 of treatment, all groups were injected intraperitoneally with 200 µL sRBC (5×10^9 cells/mL) and the treatment with BBP and BBP nanoparticles was continued for 14 days. On day 14, the thickness of hind footpad of all experimental animals was recorded using digital Plethysmometer (Ugo Basile SRL, Gemonio, Italy). The right hind footpad thickness was considered as control whereas, the left hind footpads of all mice were challenged by injecting 20 µL of sRBC (5×10^9) intradermally. After 24 hours, the thickness of footpad was measured again and the variance among right hind paw thickness and left hind paw was referred to as footpad reaction.

Measurement of serum IgG and IgM levels in response to sRBC

Commercially available ELISA kits were used to detect the serum levels of IgG and IgM. The assay was carried out using the manufacturer's protocol. To determine the level of IgM antibody, blood samples were withdrawn from all mice on day 7 and to determine the level of IgG antibody, the samples of blood were again taken from all groups of animals on day 15. Serum was rapidly separated by centrifugation at 3,500×g for 10 minutes at 4°C and stored at −20°C until used.

Statistical analysis

The results were subjected to statistical analysis using one-way ANOVA with post-Dunnett's test (to compare test samples with the control), using Graph Pad Prism 5 software (GraphPad Software, Inc., La Jolla, CA, USA) and were expressed as the mean ±SD of at least six experimental values. $P<0.001$, $P<0.01$ and $P<0.05$ were considered to be statistically significant.

Results

Preparation and physiochemical characterization of nanoparticles

The synthetic curcumin analog was successfully incorporated into PLGA-*b*-PEG nanoparticles through nanoprecipitation technique. The obtained results indicated that the average diameter, polydispersity index and zeta potential of BBP-encapsulated PLGA-*b*-PEG nanoparticles were 154.3±7.8 nm, 0.26±0.05 and −28±6.9 mV (Table 1) which are consistent with previously published work.[28] TEM analysis revealed that the nanoparticles consisted of small, discrete, spherical shaped particles as shown in Figure 2. The nanoparticle size observed in TEM was consistent with the results obtained by dynamic light scattering.

Drug entrapment and loading capacity

In our study, the entrapment of synthetic analog within the nanoparticles was found to be 79±3.60% (Table 1). This high value of EE represents that most of the drug molecules were entrapped during the formulation process as well; this high value may be attributed to the amphiphilic nature of the nanoparticles.[29] Moreover, our findings showed that BBP-encapsulated PLGA-*b*-PEG nanoparticles had a loading capacity of 32±2.7%.

Table 1 Physicochemical characterization of BBP-encapsulated PLGA-*b*-PEG nanoparticles

Particle size (nm)	Zeta potential (mV)	Polydispersity index	Entrapment efficiency (%)	Loading capacity (%)
154.3±7.8	−28±6.9	0.26±0.05	79±3.60	32±2.7

Notes: Results are presented as mean ± SD;N=3.
Abbreviations: BBP, 3,5-bis[4-(diethoxymethyl)benzylidene]-1-methyl-piperidine-4-one; PLGA-*b*-PEG, polylactic-co-glycolic acid-block-polyethylene glycol.

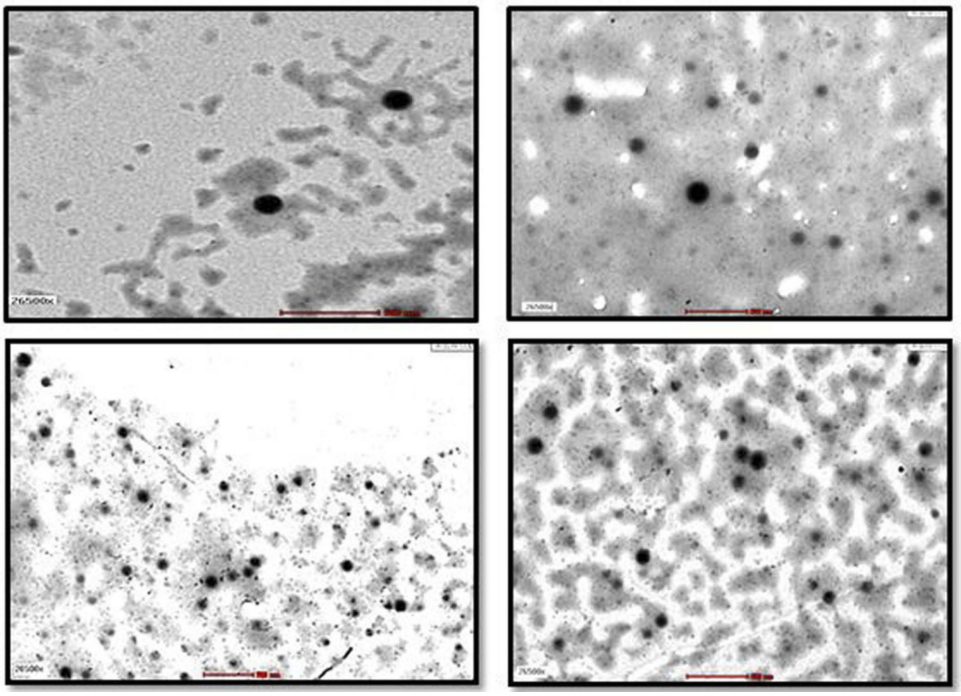

Figure 2 TEM images of BBP-encapsulated PLGA-*b*-PEG nanoparticles at a magnification of 500 nm. The scale bar or magnification is 40×.
Abbreviations: TEM, transmission electron microscope; BBP, 3,5-bis[4-(diethoxymethyl)benzylidene]-1-methyl-piperidin-4-one; PLGA-*b*-PEG, polylactic-co-glycolic acid-block-polyethylene glycol.

Drug polymer interaction

The FTIR spectra of BBP, BBP nanoparticles, and pure synthetic compound indicated that the drug was successfully encapsulated in PLGA-PEG nanoparticles and there was no interaction between the drug and the polymer (Figure 3).

In vitro release study

The percentage cumulative release of BBP alone and BBP-encapsulated nanoparticles is shown in Figure 4. A fast release of BBP was observed during first 3 hours both in acidic and basic pH which could be attributed to desorption and release of BBP from the surface of nanoparticles. After 3 hours, the drug release became slow but continuous until most of the drug was released after 48 hours. Contrary to this, for the experimental setup of BBP alone, it was noticed that the majority of the drug BBP was released within first 3 hours until the complete drug was released within 24 hours. It can be clearly seen that during the whole period of study, the release of BBP was higher at basic pH compared to acidic pH, which suggests the absorption of synthetic curcumin analog was mainly occurring in the intestine and not in the stomach.[30]

Effect of BBP and BBP nanoparticles on neutrophil migration

The results of cell migration assay showed that BBP nanoparticles exhibited dose-dependent and highly significant inhibitory effects on the directional movement of neutrophils compared to nonsensitized control (Figure 5). Also it was observed that BBP nanoparticles showed amplified immunosuppressive activity in comparison to BBP alone at all doses. However, the effects produced by BBP alone were also found significantly different when compared with control group. BBP nanoparticles at the highest dose showed comparable inhibition on the migration of neutrophils with the positive control group.

Effect of BBP and BBP nanoparticles on Mac-1 expression

Our results indicated that BBP nanoparticles showed an augmented suppression of Mac-1 expression in contrast to BBP alone. However, in comparison to the untreated group, the neutrophils purified from the blood of BBP nanoparticle-treated mice followed a dose-dependent manner of inhibition of percentage expression of CD11b/CD18, but very strong inhibitory effects

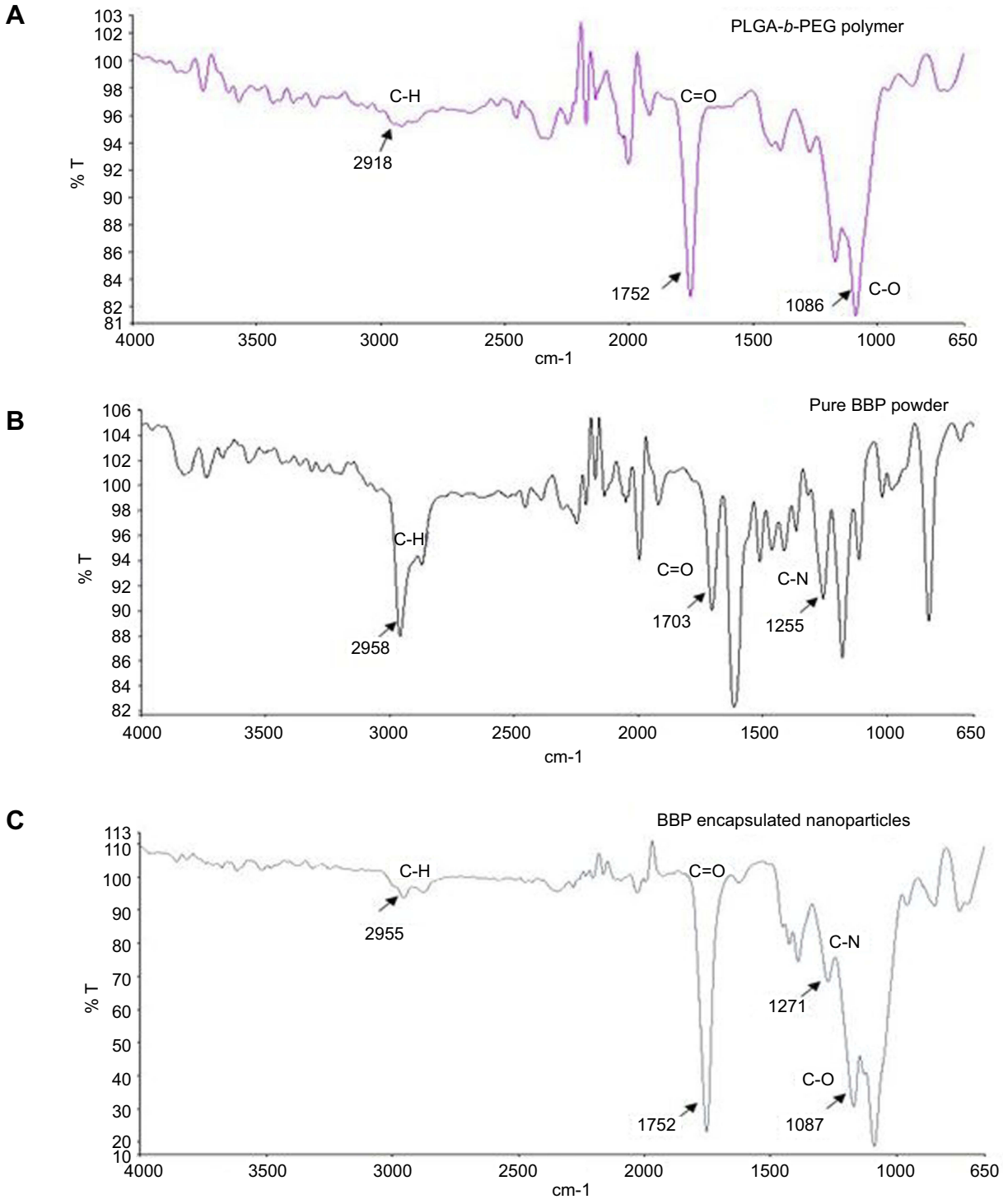

Figure 3 FTIR spectra of (**A**) PLGA-*b*-PEG polymer, (**B**) pure BBP powder and (**C**) lyophilized powder of BBP-encapsulated nanoparticles.
Abbreviations: FTIR, Fourier transform infrared spectroscopy; PLGA-b-PEG, polylactic-co-glycolic acid-block-polyethylene glycol; BBP, 3,5-bis[4-(diethoxymethyl)benzylidene]-1-methyl-piperidin-4-one; T, transmittance.

(P<0.001) were seen at the highest dose (20 mg/kg). However, significant changes were also reported at doses of 10 and 5 mg/kg (Table 2). Interestingly, it was noted that the percent inhibition of CD11b/CD18 expression by BBP nanoparticles at 5 mg/kg and BBP alone at 20 mg/kg was similar.

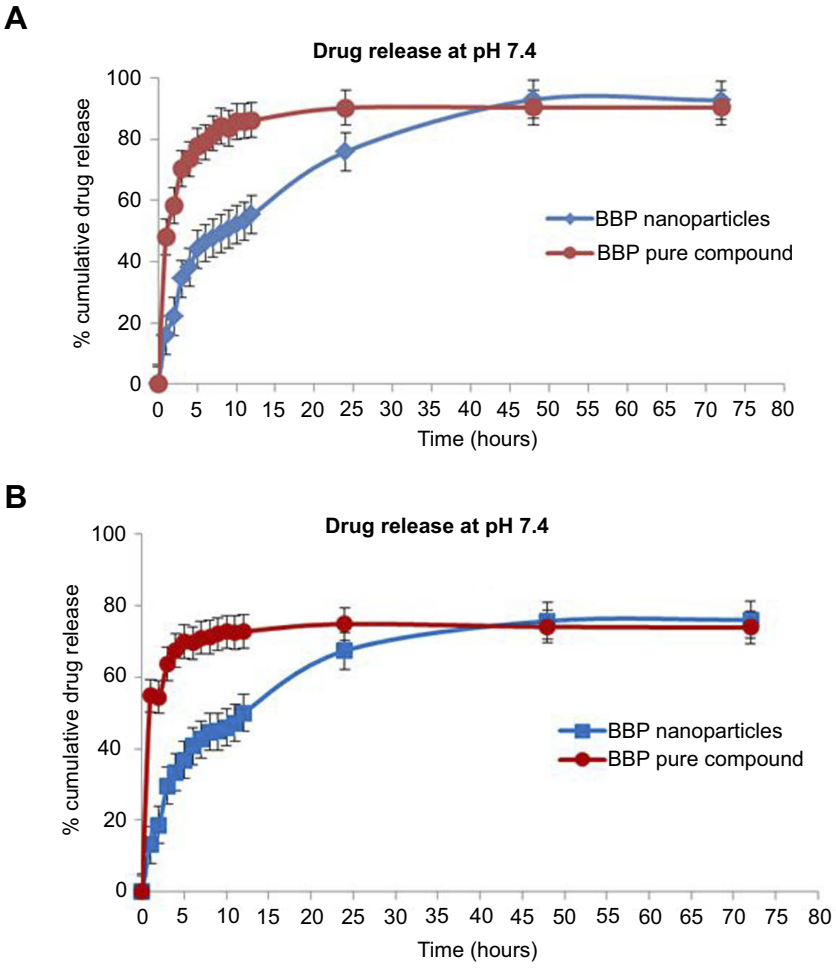

Figure 4 (**A**) In vitro release profile of BBP from lyophilized BBP-encapsulated PLGA-*b*-PEG nanoparticles at pH 2.1 and 7.4 of releasing media (**B**) In vitro release profile of pure BBP at pH 2.1 and 7.4 of releasing media.
Notes: The error bars represent the ±SD of the measurements, N=3.
Abbreviations: BBP, 3,5-bis[4-(diethoxymethyl)benzylidene]-1-methyl-piperidin-4-one; PLGA-*b*-PEG, polylactic-co-glycolic acid-block-polyethylene glycol.

Effect of BBP and BBP nanoparticles on phagocytic activity of neutrophils

A statistical summary of the potential effect of BBP nanoparticles showed that the administration of BBP nanoparticles at all doses of (5–20 mg/kg) caused the significant inhibition of bacteria engulfment by neutrophils compared to the control group (Table 2). Likewise, the suppressive activity at the highest dose of BBP nanoparticles was comparable with the positive control, cyclosporine-A. Furthermore, it can also be seen that the effect of BBP nanoparticles on the neutrophils' phagocytic activity also presented a trend of heightened suppression compared to BBP alone.

Effect of BBP and BBP nanoparticles on phagoburst activity of neutrophils

The obtained data revealed that mice treated with BBP nanoparticles and BBP alone at different doses exhibited a significant decrease in the percentage of leukocyte oxidative burst in a dose-dependent manner compared with untreated group. Although much less inhibition was observed for BBP alone at 5 mg/kg. Corresponding to Mac-1 expression activity, percent inhibition of phagoburst activity by BBP nanoparticles at 5 mg/kg and BBP alone at 20 mg/kg was found similar. In addition, a similar trend of boosted immunosuppressive effects by BBP nanoparticles was seen when compared with BBP alone (Table 2).

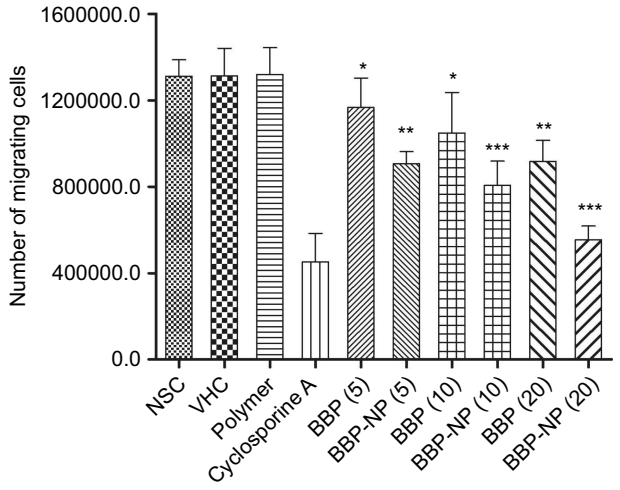

Figure 5 Effect of BBP and BBP-encapsulated nanoparticles (BBP-NP) (5, 10 and 20 mg/kg) on the chemotaxis of neutrophils isolated from experimental animals. Results are represented as mean ±SD, with N=6 in each group.
Notes: ***P<0.001; **P<0.01; *P<0.05 significantly different from the control.
Abbreviations: NSC, nonsensitized control; VHC, vehicle-treated control; polymer, PLGA-PEG; BBP, 3,5-bis[4-(diethoxymethyl)benzylidene]-1-methyl-piperidin-4-one; BBP-NP. BBP-nanoparticles.

Effect of BBP and BBP nanoparticles on plasma level of MPO enzyme

A statistical summary of the data shown in Table 3 indicated that mice treated with BBP nanoparticles and BBP alone at different doses exhibited a significant dose-dependent suppression of plasma MPO levels compared to the untreated group. The BBP nanoparticles at 20 mg/kg were found almost equally as potent as cyclosporine-A. Consistent with our previous results, nanoparticles containing BBP exhibited superior repressive effects on plasma levels of MPO compared to BBP alone in male BALB/c mice.

Effect of BBP and BBP nanoparticles on serum level of ceruloplasmin and lysozyme

The obtained data depicted that the treatment of BALB/c mice with BBP nanoparticles (5–20 mg/kg) resulted in dose-dependent and amplified inhibition of serum lysozyme and ceruloplasmin levels in contrast to the animal groups treated with BBP alone (Table 3). Along with this, it was also noticeable that in comparison to the untreated group, the inhibitory response produced by BBP-encapsulated nanoparticles and BBP alone on both ceruloplasmin and lysozyme levels in the serum was significantly different.

Effect of BBP and BBP nanoparticles on splenocyte proliferation

The results revealed that the synthetic analog encapsulated nanoparticles provoked highly significant inhibition on Con-A and LPS induced splenic lymphocyte proliferation in contrast to sensitized control and this inhibition was observed in a dose-dependent way. The reduced proliferative responses of BBP nanoparticles on both T cell and B cell were comparable with the cyclosporine-A-treated group. However, it was also noted that the antiproliferative effects of BBP alone elicited significant inhibition only at the highest dose (20 mg/kg) compared to untreated the group. The comparison between BBP alone and BBP nanoparticles exposed the increased antiproliferative activity by nanoparticles containing synthetic compound (Table 4).

Table 2 Effect of BBP and BBP-encapsulated nanoparticles on percent Mac-1 activity, percent phagocytic activity and percent phagoburst activity

Groups	Treatment	Dose (mg/kg)	Percent Mac-1 expression	Percent Phagocytic activity	Percent Phagoburst activity
I	NSC	–	85.16±4.8	73.98±4.7	81.47±3.4
II	VHC	-	83.76±5.5	75.04±3.4	83.92±3.7
III	Polymer		82.76±3.4	75.87±3.3	82.71±3.4
IV	Cyclosporine-A	20	66.69±4.3***	45.29±5.9***	63.74±4.2***
V	BBP	5	82.22±5.4	69.08±5.4	80.70±3.5
VI	BBP-NP	5	75.09±3.3**	59.71±3.2**	70.38±4.6**
VII	BBP	10	79.19±6.1	65.53±4.2	75.96±3.6
VIII	BBP-NP	10	72.04±3.9**	56.31±4.5***	68.65±2.5***
IX	BBP	20	75.79±3.6**	63.13±3.3*	70.21±5.2**
X	BBP-NP	20	68.75±5.0***	51.74±4.4***	64.57±3.7***

Notes: Results are presented as mean ±SD values. ***P<0.001; **P<0.01; *P<0.05 are significantly different compared with the control group.
Abbreviations: BBP, 3,5-bis[4-(diethoxymethyl)benzylidene]-1-methyl-piperidin-4-one; NSC, nonsensitized control; VHC, vehicle-treated control; polymer, PLGA-PEG; BBP-NP, BBP-nanoparticles.

Table 3 Effect of BBP and BBP-encapsulated nanoparticles on MPO plasma levels and serum levels of lysozyme and ceruloplasmin

Groups	Treatment	Dose (mg/kg)	MPO plasma levels (ng/mL)	Lysozyme levels (ng/mL)	Ceruloplasmin levels (ng/mL)
I	NSC	-	81.57±8.5	1230±72.1	132.0±13.1
II	VHC	-	80.78±6.5	1233±80.3	144.4±10.8
III	Polymer		82.85±6.4	1239±82.9	137.0±9.3
IV	Cyclosporine-A	20	28.17±6.6***	814.3±56.4***	82.62±8.7***
V	BBP	5	70.70±7.9	1067±57.69	122.2±12.4
VI	BBP-NP	5	55.32±4.8**	965.9±56.7*	107.7±8.3*
VII	BBP	10	63.03±6.7	1044±46.5	117.3±6.6
VIII	BBP-NP	10	42.57±6.5***	898.8±41.4**	98.97±8.9**
IX	BBP	20	48.62±4.8**	976.2±56.0*	110.6±8.9*
X	BBP-NP	20	32.40±4.7***	838.5±54.2***	91.65±7.2***

Notes: Results are presented as mean ±SD values. ***P<0.001; **P<0.01; *P<0.05 are significantly different compared with the control group.
Abbreviations: BBP, 3,5-bis[4-(diethoxymethyl)benzylidene]-1-methyl-piperidin-4-one; MPO, myeloperioxidase; NSC, nonsensitized control; VHC, vehicle-treated control; polymer, PLGA-PEG; BBP-NP, BBP-nanoparticles.

Table 4 Effect of BBP and BBP-encapsulated nanoparticles on proliferation of T and B lymphocytes (SI) and percent expression of $CD4^+$ and $CD8^+$ cells in the spleen

			Lymphocyte proliferation (SI)		T- cell subset detection (%)	
Groups	Treatment	Dose (mg/kg)	T cells	B cells	$CD4^+$	$CD8^+$
I	SC	–	3.72±0.3	2.52±0.4	25.87±3.7	34.28±5.0
II	VHC	–	3.56±0.5	2.63±0.5	26.67±4.7	33.37±4.7
III	Polymer		3.61±0.5	2.40±0.7	26.08±6.2	33.40±4.2
IV	Cyclosporine-A	20	1.44±0.4***	0.98±0.6***	9.79±4.4***	14.97±4.8***
V	BBP	5	3.11±0.6	2.00±0.5	21.62±4.5	30.08±3.5
VI	BBP-NP	5	1.76±0.1**	1.25±0.2**	15.83±4.5*	23.90±4.2*
VII	BBP	10	2.82±0.3	1.71±0.4	18.43±3.2	27.07±4.6
VIII	BBP-NP	10	1.52±0.1**	1.12±0.3**	13.40±4.2**	20.83±3.7*
IX	BBP	20	2.50±0.5*	1.45±0.5*	15.00±4.1	25.47±4.7
X	BBP-NP	20	1.32±0.1***	0.97±0.3***	11.68±5.0***	15.00±5.7***

Notes: Results are presented as mean ±SD values. ***P<0.001; **P<0.01; *P<0.05 are significantly different compared with the control group.
Abbreviations: BBP, 3,5-bis[4-(diethoxymethyl)benzylidene]-1-methyl-piperidin-4-one; SI, stimulation index; SC, sensitized control; VHC, vehicle treated control; polymer, PLGA-PEG; BBP-NP, BBP-nanoparticles.

Effect of BBP and BBP nanoparticles on lymphocyte phenotyping

The data shown in Table 4 revealed that in comparison to the sensitized control group, the percentage expression of $CD4^+$ and $CD8^+$ was significant and dose-dependently suppressed at graded doses by BBP as well as BBP nanoparticles. However, the inhibition by BBP nanoparticles at 20 and 10 mg/kg doses was found comparable to the immunosuppressant drug. Likewise, it can be seen that the nanoparticles containing BBP improved the inhibitory activity on lymphocyte phenotyping compared to the effects when BBP was administered alone.

Effect of BBP and BBP nanoparticles on serum level of IL-2, IL-4 and IFN-γ

The results revealed that in comparison to the sensitized control group, the sera level of IL-2 and IL-4 fed with BBP nanoparticles were remarkably reduced and the effect seemed comparable to the cyclosporine-A treated group at a dose of 20 mg/kg as shown in Figure 6A and 6C. On the contrary, Figure 6B presented that the sera level of Th1 cytokine, INF-γ were found to be significantly suppressed at all doses when compared to the sensitized control group. However, at the highest dose, the strongest inhibitory effects were seen, suggesting that BBP-encapsulated nanoparticles were as efficacious as the positive control,

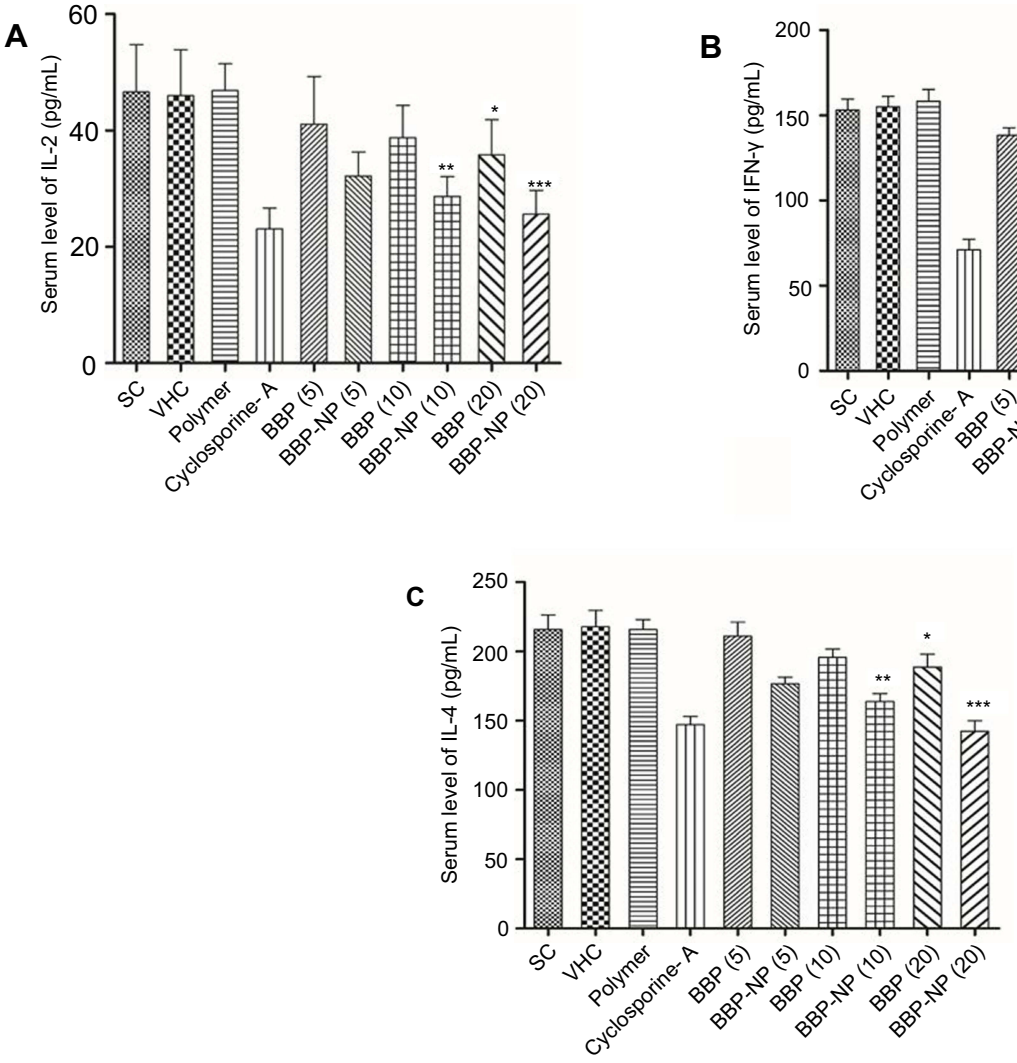

Figure 6 Effect of BBP and BBP-encapsulated nanoparticles (BBP-NP) (5, 10 and 20 mg/kg) on the serum level of (**A**) IL-2, (**B**) IL-4 and (**C**) IFN-γ from experimental animals. Results are represented as mean ±SD, with n=6 in each group. ***P<0.001; **P<0.01; *P<0.05 significantly different from the control.
Abbreviations: IL, interleukin; IFN, interferon; SC, sensitized control; VHC, vehicle-treated control; polymer, PLGA-PEG; BBP, 3,5-bis[4-(diethoxymethyl)benzylidene]-1-methyl-piperidin-4-one; BBP-NP. BBP-nanoparticles.

cyclosporine-A. A comparative analysis between the BBP nanoparticles and the BBP-alone treated group exposed that BBP nanoparticles provoked amplified repressive effects signifying the improved immunosuppressive potential.

Effect of BBP and BBP nanoparticles on delayed type hypersensitivity response

In this study, the immunized treated groups administered with BBP-encapsulated nanoparticles and BBP alone at graded doses were found to elicit substantial suppression in paw edema compared to the untreated group at 24 hours. However, as can be seen in Table 5, the percentage inhibition in the paw edema by BBP nanoparticles was more pronounced in contrast to BBP alone. BBP nanoparticles at 20 mg/kg displayed comparable immunosuppressive effects with cyclosporine-A.

Effect of BBP and BBP nanoparticles on serum level of IgG and IgM antibodies

The levels of immunoglobulins IgG showed a highly significant reduction (in a dose-dependent manner) in sera of BBP nanoparticles treated mice when compared to the control, but fewer suppressive effects were noticed in sera of BBP-alone treated mice (Table 5). Similarly, the

Table 5 Effect of BBP and BBP-encapsulated nanoparticles on DTH response and serum IgM and IgG levels in BALB/c mice

			Paw thickness (mm)		Production of immunoglobulins (U/mL)	
Groups	**Treatment**	**Dose (mg/kg)**	**24 hours oedema**	**Percent inhibition in paw edema**	**IgM**	**IgG**
I	SC	–	0.74±0.1		46.72±5.4	81.10±7.2
II	VHC	–	0.76±0.5		45.62±3.8	80.55±6.0
III	Polymer		0.73±0.4		45.23±6.3	79.05±5.4
IV	Cyclosporine-A	20	0.44±0.4	40.54***	21.44±5.0***	36.92±5.2***
V	BBP	5	0.68±0.6	8.1*	43.00±5.1	75.68±7.1
VI	BBP-NP	5	0.55±0.3	25.67**	31.22±5.2**	61.59±5.7**
VII	BBP	10	0.64±0.5	13.51**	39.91±4.4	71.23±5.2
VIII	BBP-NP	10	0.51±0.3	31.08**	28.17±2.8**	49.92±5.3**
IX	BBP	20	0.61±0.3	17.56**	34.13±6.3*	68.72±5.3*
X	BBP-NP	20	0.49±0.5	33.78***	24.79±6.5***	40.09±3.9***

Notes: Results are presented as mean ±SD values. ***P<0.001; **P<0.01; *P<0.05 are significantly different compared with the control group.
Abbreviations: BBP, 3,5-bis[4-(diethoxymethyl)benzylidene]-1-methyl-piperidin-4-one; BBP-NP, BBP-nanoparticles; DTH, delayed type hypersensitivity; Ig, immunoglobulin; SC, sensitized control; VHC, vehicle-treated control; polymer, PLGA-PEG.

reduction in sera levels of IgM antibody were found significantly different for both BBP and its nanoparticles-treated group when compared with the untreated sensitized group. Additionally, the data revealed that BBP nanoparticles produced comparable suppressive effects on serum levels of IgG and IgM with cyclosporine-A at the highest dose.

Discussion

This study was designed to investigate the immunosuppressive effects of PLGA-PEG nanoparticles containing the synthetic curcumin analog, BBP compared to the effects produced by the synthetic compound alone. The findings of this study suggest that the immunosuppressive effects of BBP were enhanced as PLGA-*b*-PEG nanoparticles. The curcumin analog-encapsulated PLGA-PEG nanoparticles were successfully prepared. The mixture of amphiphilic block polymer and BBP when added dropwise to the aqueous phase, the hydrophobic domain of PEG-*b*-PLGA, ie, PLGA, formed a hydrophobic core with BBP being encapsulated while the hydrophilic domain, PEG, remained on the surface of the polymeric nanoparticles and stabilized the nanoparticles size.[31] The size of nanoparticles plays a fundamental role as it affects the biodistribution profile and in vivo efficacy and the optimal size of nanoparticles for in vivo application lies between 70 and 200 nm.[32] The high value of zeta potential obtained in this study showed that the nanoparticles prepared were nonaggregated and physically stable.[33] Evidenced by a number of previous studies, it has been demonstrated that most of the nanoparticles developed for the drug delivery system are spherical in shape.[34] In addition, BBP-encapsulated in PLGA-PEG nanoparticles have shown a sustained release, which can be explained by the fact that the release kinetics were entirely controlled by diffusion.[35]

The immunosuppressive effects of BBP and BBP-encapsulated nanoparticles on the nonspecific immune responses involved the phagocytosis process. For the significant reduced percentage of CD11b and CD18 expressions compared with the control group, it is assumed that BBP and BBP nanoparticles may have a direct effect on signal transduction or translocation pathways and conformational changes on CD11b/CD18 complexes as neutrophils; once activated CD11b/CD18 are translocated to the cell surface presumably through conformational or topological alterations.[36] In addition, the downregulation of Mac-1 could be one of the possible mechanism for the inhibition of FBS-induced chemotaxis of neutrophils isolated from mice pretreated with BBP and BBP nanoparticles because chemoattractant-triggered neutrophil's chemotaxis is mediated by Mac-1.[37] A recent study revealed that the inhibition of Mac-1 expression caused the antibodies against the complementary surface receptors, CR3 on neutrophils to suppress the binding of microbes to phagocytes.[38] Another study described that suppression of CD11b/CD18 results in impaired degranulation and superoxide production in peritonitis models as well as decreased adhesion, and also causes impairment of both spreading and phagocytosis of complementary opsonized particles.[39] MPO, being part of the innate immune system, plays an important role in cellular homeostasis and impaired levels cause initiation and

progression of acute and chronic inflammatory diseases.[40] The substantial inhibition of MPO could be attributed to the inhibition of Mac-1, as the downregulation of Mac-1 suppresses the sequential phagocytosis process and release of toxic radicals and enzymes. Lysozyme enzyme triggers the complement system through its bactericidal and opsonin effects to prevent different infections[41] and ceruloplasmin is an important component of cell-mediated immunity.[42] The potential inhibitory effects of BBP and its nanoparticles at the indicated doses on lysozyme serum levels could possibly be due to inhibition of the phagocytosis process. The aforesaid enzyme was released during the process of phagocytosis while the dose-dependent inhibition of ceruloplasmin levels could be attributed to the suppression of certain pro-inflammatory cytokines like TNF-α, IL-1 and IL-6 which cause the release of ceruloplasmin.[43]

The suppression of T cell-mediated immune functions occupies a key position in the pathological process of different chronic inflammatory disorders. The substantial reduction of T and B cell proliferation could be attributed to the antiproliferative action of the BBP nanoparticles on the inhibition of enzymes (ribonucleotide reductase and DNA polymerase) involved in process of DNA synthesis or it may have repressed the growth of cells during the S phase of cell cycle.[44] The mechanism was further elucidated by investigating the effects of BBP and BBP nanoparticles on the differentiation of T lymphocytes into $CD4^+$ and $CD8^+$ cell subsets in sRBC challenged male BALB/c mice and our results corroborated previously reported work.[45] T cell-mediated immunological responses were also explored by the release of Th1 and Th2 cytokines and it is suggested that the reduced production of cytokines may be due to the inhibition of T and B cells documented in this study. In addition, it also has been reported that production of IL-12 is one of the major mechanisms that affects the cytokine production in $CD4^+$ cells.[46] DTH is one of the important cell-mediated immune responses and has been reported to provide protection against several intracellular pathogens. The possible mechanism for substantial inhibition of the paw edema at the highest dose (20 mg/kg) could be due to the inhibition of T lymphocytes activation and the resultant release of cytokines.[47] T and B cells along with the macrophages are involved in the production of immunoglobulins. Numerous studies reported that the reduction in humoral immune responses could be due to suppression of antigen processing and presentation, or the inhibition of proliferation of T and B cells or might be influenced by the release of different cytokines produced upon T cell and B cell stimulation.[48]

Therefore, the findings from this study revealed that the synthetic analog, BBP-encapsulated PLGA-b-PEG nanoparticles displayed immunosuppressive effects as strong as cyclosporine-A as well as exhibiting superior biological activity in comparison to BBP alone on various cellular and humoral parameters of immune responses. Thus, polymeric nanoparticles, when fabricated as drug carriers for encapsulated BBP, elicited enhanced immunosuppressive effects in male BALB/c mice. Previously, one study reported the enhanced hepatoprotective effects of bis-demethoxy curcumin analog (BDMC) nanoparticles compared to free drug.[49] Similarly, BDMC curcumin analog nanoparticles have shown potent anticancer activity.[50] Another study showed the enhanced inhibitory effects of curcumin-loaded PLGA-PEG nanoparticles on breast cancer cell lines compared to curcumin alone.[51] The increased suppressive effects could be attributed to the long-term systemic circulation provided by PLGA-*b*-PEG nanoparticles as PEG reduces the interactions between the nanoparticles and the enzymes of the digestive fluids and increases the uptake of the drug in the bloodstream and lymphatic tissue.[52] In addition, the stealth behavior of PEG could possibly reduce the clearance of BBP-encapsulated nanoparticles by reticulo-endothelial system and increase in vivo circulation time, thus allowing the drug to reach its site of action.[53] The mechanism of increased efficacy of the nanoparticles could also be attributed to better internalization and endocytosis of the nanoparticles by the cells.

Conclusion

In conclusion, we reported the preparation and physicochemical characterization of BBP-encapsulated PLGA-*b*-PEG nanoparticles with enhanced therapeutic effects on the cellular and humoral components of the innate and adaptive immune system of male BALB/c. Our present work and prior study in combination with the observation corroborated that modification of structural features along with the provision of novel drug delivery system can increase the *in vivo* therapeutic effectiveness of a hydrophobic and least bioavailable drug like curcumin. However, it is strongly recommended that detailed studies should be undertaken to explore the mechanism behind the increased efficacy of BBP nanoparticles as well as absorption, and pharmacokinetic properties of BBP and BBP nanoparticles, in particular, need to be identified.

Acknowledgments

The authors thank Universiti Kebangsaan Malaysia (UKM) for providing the grant under Dana Impak Perdana (grant number DIP-2015-013).

Disclosure

The authors report no conflicts of interest in this work.

References

1. Arshad L, Haque MA, Bukhari SNA, Jantan I. An overview of structure–activity relationship studies of curcumin analogs as antioxidant and anti-inflammatory agents. *Future Med Chem*. 2017;9(6):605–626.
2. Aggarwal BB, Sung B. Pharmacological basis for the role of curcumin in chronic diseases: an age old spice with modern targets. *Trends Pharmacol Sci*. 2009;30(2):85–94. doi:10.1016/j.tips.2008.11.002
3. Aggarwal BB, Harikumar KB. Potential therapeutic effects of curcumin, the anti-inflammatory agent, against neurodegenerative, cardiovascular, pulmonary, metabolic, autoimmune and neoplastic diseases. *Int Biochem Cell Biol*. 2009;41(1):40–59. doi:10.1016/j.biocel.2008.06.010
4. Mohanty C, Sahoo SK. The *in vitro* stability and *in vivo* pharmacokinetics of curcumin prepared as an aqueous nanoparticulate formulation. *Biomaterials*. 2010;31(25):6597–6611. doi:10.1016/j.biomaterials.2010.04.062
5. Jurenka JS. Anti-inflammatory properties of curcumin, a major constituent of *Curcuma longa*: a review of preclinical and clinical research. *Altern Med Rev*. 2009;14(2):141–153.
6. Gordon ON, Luis PB, Sintim HO, Schneider C. Unraveling curcumin degradation autoxidation proceeds through spiroepoxide and vinylether intermediates en route to the main bicyclopentadione. *J Biol Chem*. 2015;290(8):4817–4828. doi:10.1074/jbc.M114.618785
7. Mock CD, Jordan BC, Selvam C. Recent advances of curcumin and its analogues in breast cancer prevention and treatment. *RSC Adv*. 2015;5(92):75575–75588. doi:10.1039/C5RA14925H
8. Mehanny M, Hathout RM, Geneidi AS, Mansour S. Studying the effect of physically-adsorbed coating polymers on the cytotoxic activity of optimized bisdemethoxycurcumin loaded-PLGA nanoparticles. *J Biomed Mater Res B*. 2017;105(5):1433–1445. doi:10.1002/jbm.a.36028
9. Mehanny M, Hathout RM, Geneidi AS, Mansour S. Exploring the use of nanocarrier systems to deliver the magical molecule; curcumin and its derivatives. *J Control Release*. 2016;10(225):1–30. doi:10.1016/j.jconrel.2016.01.018
10. Hathout RM, Al-Ahmady SH, Metwally AA. Curcumin or bisdemethyoxycurcumin for nose-to-brain treatment of Alzheimer disease? A bio/chemo-informatics case study. *Nat Prod Res*. 2017. doi:10.1080/14786419.2017.1385017
11. Farid MM, Hathout RM, Fawzy M, Abou-Aisha K. Silencing of the scavenger receptor (Class B–type 1) gene using siRNA-loaded chitosan nanaoparticles in a HepG2 cell model. *Colloids Surf B Biointerfaces*. 2014;123:930–937. doi:10.1016/j.colsurfb.2014.10.045
12. El-Marakby EM, Hathout RM, Taha I, Mansour S, Mortada ND. A novel serum-stable liver targeted cytotoxic system using valerate-conjugated chitosan nanoparticles surface decorated with glycyrrhizin. *Int J Pharm*. 2017;525(1):123–138. doi:10.1016/j.ijpharm.2017.03.081
13. Bisht S, Maitra A. Systemic delivery of curcumin: 21st century solutions for an ancient conundrum. *Curr Drug Discov Technol*. 2009;6(3):192–199.
14. Knop K, Hoogenboom R, Fischer D, Us S. Poly (ethylene glycol) in drug delivery: pros and cons as well as potential alternatives. *Angew Chem Int Ed*. 2010;49(36):6288–6308. doi:10.1002/anie.200902672
15. Oupicky D, Ogris M, Howard KA, Dash PR, Ulbrich K, Seymour LW. Importance of lateral and steric stabilization of polyelectrolyte gene delivery vectors for extended systemic circulation. *Mol Ther*. 2002;5(4):463–472. doi:10.1006/mthe.2002.0568
16. Arshad L, Jantan I, Bukhari SNA, et al. Inhibitory effects of α, β-unsaturated carbonyl-based compounds and their pyrazoline derivatives on the phagocytosis of human neutrophils. *Med Chem Res*. 2018;27(5):1460–1471.
17. Arshad L, Jantan I, Bukhari SNA, Fauzi M. 3, 5-Bis [4-(diethoxymethyl) benzylidene]-1-methyl-piperidin-4-one, a novel curcumin analogue, inhibits cellular and humoral immune responses in male Balb/c mice. *Curr Pharm Biotechnol*. 2018;19(468–482). doi:10.2174/1389201019666181022115405
18. Fessi H, Puisieux F, Devissaguet J, Ammoury N, Benita S. Nanocapsule formation by interfacial polymer deposition following solvent displacement. *Int J Pharm*. 1989;55:R1–R4. doi:10.1016/0378-5173(89)90281-0
19. Jin H, Pi J, Zhao Y, et al. EGFR-targeting PLGA-PEG nanoparticles as a curcumin delivery system for breast cancer therapy. *Nanoscale*. 2017;9(42):16365–16374. doi:10.1039/c7nr06898k
20. Thomson A, Whiting P, Simpson J. Cyclosporine: immunology, toxicity and pharmacology in experimental animals. *Agents Actions*. 1984;15(3–4):306–327.
21. Borel JF, Feurer C, Magnee C, Stähelin H. Effects of the new anti-lymphocytic peptide cyclosporin A in animals. *Immunol*. 1977;32(6):1017–1025.
22. Kumar S, Jyoti A, Keshari RS, Singh M, Barthwal MK, Dikshit M. Functional and molecular characterization of NOS isoforms in rat neutrophil precursor cells. *Cytom A*. 2010;77(5):467–477.
23. Ilangkovan M, Jantan I, Mesaik MA, Bukhari SNA. Immunosuppressive effects of the standardized extract of *Phyllanthus amarus* on cellular immune responses in Wistar-Kyoto rats. *Drug Des Develop Ther*. 2015;9:4917–4930.
24. Ahmad W, Jantan I, Kumolosasi E, Bukhari SNA. Immunostimulatory effects of the standardized extract of *Tinospora crispa* on innate immune responses in Wistar Kyoto rats. *Drug Des Develop Ther*. 2015;9:2961–2973.
25. Varalakshmi C, Ali AM, Pardhasaradhi B, et al. Immunomodulatory effects of curcumin *in vivo*. *Inter Immunopharmacol*. 2008;8(5):688–700. doi:10.1016/j.intimp.2008.01.008
26. Gupta A, Khajuria A, Singh J, et al. Immunomodulatory activity of biopolymeric fraction RLJ-NE-205 from Picrorhiza kurroa. *Int Immunopharmacol*. 2006;6(10):1543–1549. doi:10.1016/j.intimp.2006.05.002
27. Koffuor GA, Amoateng P, Andey TA. Immunomodulatory and erythropoietic effects of aqueous extract of the fruits of *Solanum torvum* Swartz (Solanaceae). *Pharmacogn Res*. 2011;3(2):130. doi:10.4103/0974-8490.81961
28. Dao TPT, Nguyen TH, Ho TH, et al. A new formulation of curcumin using poly (lactic-co-glycolic acid)—polyethylene glycol diblock copolymer as carrier material. *Adv Nat Sci*. 2014;5(3):035013.
29. Missirlis D, Hubbell J, Tirelli N. Thermally-induced glass formation from hydrogel nanoparticles. *Soft Matter*. 2006;2(12):1067–1075. doi:10.1039/b607437e
30. Xie X, Tao Q, Zou Y, et al. PLGA nanoparticles improve the oral bioavailability of curcumin in rats: characterizations and mechanisms. *J Agric Food Chem*. 2011;59(17):9280–9289. doi:10.1021/jf202135j
31. Karve S, Werner ME, Cummings ND, et al. Formulation of diblock polymeric nanoparticles through nanoprecipitation technique. *J Vis Exp: JoVE*. 2011;55.

32. Owens DE III, Peppas NA. Opsonization, biodistribution, and pharmacokinetics of polymeric nanoparticles. *Inter J Pharm*. 2006;307(1):93–102. doi:10.1016/j.ijpharm.2005.10.010
33. Müller RH. *Colloidal Carriers for Controlled Drug Delivery and Targeting: Modification, Characterization and In Vivo Distribution*. Stutgart, Germany: Taylor & Francis, Wissenschaftliche Verlagsgesellschaft; 1991. 227 figures.
34. Dandekar PP, Jain R, Patil S, et al. Curcumin-loaded hydrogel nanoparticles: application in anti-malarial therapy and toxicological evaluation. *J Pharm Sci*. 2010;99(12):4992–5010. doi:10.1002/jps.22191
35. Tang L, Azzi J, Kwon M, et al. Immunosuppressive activity of size-controlled PEG-PLGA nanoparticles containing encapsulated cyclosporine A. *J Transpl*. 2012;2012.
36. Yoshida N, Yoshikawa T, Tanaka Y, et al. A new mechanism for anti-inflammatory actions of proton pump inhibitors–inhibitory effects on neutrophil endothelial cell interactions. *Alimen Pharmacol Ther*. 2000;14(s1):74–81. doi:10.1046/j.1365-2036.2000.014s1074.x
37. Ley K, Laudanna C, Cybulsky MI, et al. Getting to the site of inflammation: the leukocyte adhesion cascade updated. *Nat Rev Immunol*. 2007;7(9):678. doi:10.1038/nri2156
38. Burg ND, Pillinger MH. The neutrophil: function and regulation in innate and humoral immunity. *Clin Immunol*. 2001;99(1):7–17. doi:10.1006/clim.2001.5007
39. Olza J, Aguilera CM, Gil-Campos M, et al. Myeloperoxidase is an early biomarker of inflammation and cardiovascular risk in prepubertal obese children. *Diabetes Care*. 2012;35(11):2373–2376. doi:10.2337/dc12-0614
40. Kim EK, Choi E-J. Pathological roles of MAPK signaling pathways in human diseases. *Biochim Biophys Acta*. 2010;1802(4):396–405. doi:10.1016/j.bbadis.2009.12.009
41. Rodríguez MC, Rivas GA. Label-free electrochemical aptasensor for the detection of lysozyme. *Talanta*. 2009;78(1):212–216. doi:10.1016/j.talanta.2008.11.002
42. Wang H, Wang M, Chen J, et al. A polysaccharide from Strongylocentrotus nudus eggs protects against myelosuppression and immunosuppression in cyclophosphamide-treated mice. *Int Immunopharmacol*. 2011;11(11):1946–1953. doi:10.1016/j.intimp.2011.06.006
43. De la Fuente M, Victor V. Anti-oxidants as modulators of immune function. *Immunol Cell Biol*. 2000;78(1):49–54. doi:10.1046/j.1440-1711.2000.00884.x
44. Luckheeram RV, Zhou R, Verma AD, et al. CD4(+)T cells: differentiation and functions. *Clin Develop Immunol*. 2012;2012:925135. doi:10.1155/2012/925135
45. Farrar JD, Asnagli H, Murphy KM. T helper subset development: roles of instruction, selection, and transcription. *J Clin Investig*. 2002;109(4):431–435. doi:10.1172/JCI15093
46. Akagawa KS, Tokunaga T. Delayed-Type Hypersensitivity (DTH) in BCG-Sensitized Mice. *Microbiol Immunol*. 1979;23(5):403–414.
47. Benacerraf B. Opinion: a hypothesis to relate the specificity of T lymphocytes and the activity of I region-specific Ir genes in macrophages and B lymphocytes. *J Immunol*. 1978;120(6):1809–1812.
48. Amirghofran Z, Azadmehr A, Javidnia K. *Haussknechtia elymatica*: a plant with immunomodulatory effects. *Iran J Immunol*. 2007;4(1):26–31.
49. Anuradha C, Aukunuru J. Preparation, characterisation and *in vivo* evaluation of bis-demethoxy curcumin analogue (BDMCA) nanoparticles. *Trop J Pharm Res*. 2010;9:51–58. doi:10.4314/tjpr.v9i1.52036
50. Francis AP, Murthy PB, Devasena T. Bis-demethoxy curcumin analog nanoparticles: synthesis, characterization, and anticancer activity *in vitro*. *J Nanosci Nanotechnol*. 2014;14:4865–4873.
51. Anand P, Thomas SG, Kunnumakkara AB, et al. Biological activities of curcumin and its analogues (congeners) made by man and mother nature. *Biochem Pharmacol*. 2008;76:1590–1611. doi:10.1016/j.bcp.2008.08.008
52. Tobıo M, Sanchez A, Vila A, et al. The role of PEG on the stability in digestive fluids and *in vivo* fate of PEG-PLA nanoparticles following oral administration. *Colloids Surf B*. 2000;18:315–323. doi:10.1016/S0927-7765(99)00157-5
53. Muthu M. Nanoparticles based on PLGA and its co-polymer: an overview. *Asian J Pharm*. 2009;3:266–273. doi:10.4103/0973-8398.59948